JOURNAL OF MATERIALS SCIENCE 20 (1985) 1321–1332

# High-temperature deformation of a polycrystalline alumina containing an intergranular glass phase

D. R. CLARKE
*Thomas J. Watson Research Center, IBM, Yorktown Heights, New York 10598, USA*

The high-temperature creep and flexural deformation of a model alumina-glass ceramic is reported over the temperature range in which the glass phase softens (from a viscosity of $\sim 10^7$ to $\sim 10^3$ P). Under both loading conditions the deformation is accompanied by extensive cavitational damage throughout the material. The cavitation is inhomogeneously distributed and at high stresses can be localized into bands. In addition, crack propagation at high temperature results in the formation of a cavitational zone on either side of the fracture and measurements of its size are presented as a function of deformation temperature. On the basis of the microstructural observations of the deformed material, the sequence by which isolated cavities grow and link up prior to failure, is described.

## 1. Introduction

Intergranular glass phases are present in many structural ceramics and it is now recognized that they can adversely affect the strength and structural integrity of this class of material at high temperature. In a number of ceramics, for instance hot-pressed or sintered silicon nitride and debased aluminas, the glass is a residual phase formed from the additives used to promote densification by liquid-phase sintering. In other materials, prepared by the controlled crystallization of a glass (glass-ceramics), the presence of an intergranular glass phase is a consequence of incomplete crystallization. In still other materials, an intergranular glass phase is formed from a liquid phase produced by the reaction between the ceramic and any impurities present. The latter tend to be principally silica-based but phosphate-based intergranular phases have recently been detected in nuclear-waste ceramics. In addition, as the microstructures of ceramics are examined in the greater detail afforded by transmission electron microscopy techniques, developed for the detection of intergranular glass phases having thicknesses of $\sim 0.3$ nm or greater, more examples of this class of ceramic are being identified.

At temperatures above what is presumed to be the softening point of the intergranular phase, the mechanical properties can no longer be characterized as being brittle: the modulus of rupture is temperature dependent; the materials deform in creep; creep crack growth appears to be thermally activated and cavitation in the intergranular phase is observable. The behaviour of materials in this temperature regime has been documented in the last decade, principally for silicon nitride alloys, hot-pressed aluminas and glass-ceramics. Unfortunately, the materials studied have, with few exceptions and despite considerable effort, been poorly characterized particularly in regard to the properties of the intergranular glass phase. This is especially true of the glass in the silicon nitride materials but also pertains to the other materials. The task is a formidable one, requiring not only a knowledge of the composition of the intergranular phase but also properties such as viscosity, diffusivities and solubility (of the crystalline phase) in the glass phase. Using such data in modelling the high-temperature properties also necessitates the assumption that macroscopically determined parameters pertain to the properties of constrained intergranular phases that, in some materials such as hot-pressed silicon nitride, are only 1 to 2 nm thick. Whilst the latter

0022–2461/85 $03.00 + .12  

problem cannot be directly tackled, the determination of the pertinent data concerning the properties of the intergranular phase can be circumvented by fabricating a ceramic from a mixture of crystalline and non-crystalline components, the properties of each of which are already known. This approach is adopted in the present, experimental investigation.

Accordingly, the present work was undertaken on an alumina ceramic containing a glass phase of a commercial composition whose properties are well documented. The objective being two-fold: first, to provide data on selected high-temperature deformation properties; second, to identify on the basis of microstructural observations, the deformation mechanisms operating. Together, this provides a first step in a systematic characterization of the high-temperature deformation behaviour of structural ceramics containing an intergranular glass phase and also provide experimental data for theoretical models being developed.

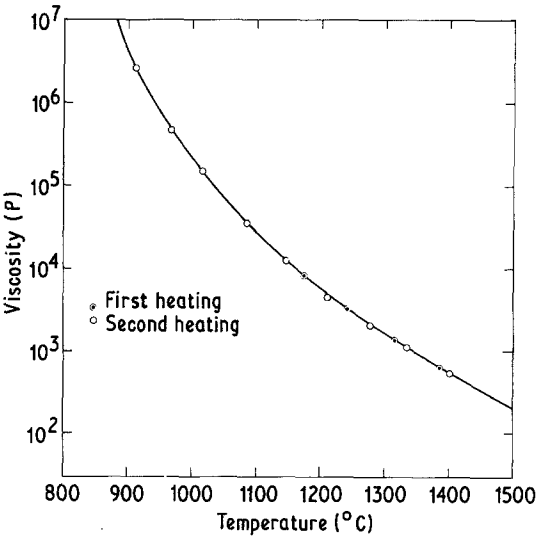


*Figure 1* Viscosity of the Corning 7059 glass used to form the intergranular phase in the alumina composites. (After Corning Glass Works.)

## 2. Materials and microstructure

### 2.1. Material

The composite material was prepared by hot-pressing alpha alumina powder and 10 vol% powdered Corning 7059 glass at 1550° C for 2 h in graphite dies. An all oxide system was chosen so that the deformation experiments could be performed in air. The 7059 glass, a strontium, barium-rich alumino-silicate glass, was selected as it contains a relatively high concentration of high atomic weight elements affording good atomic number contrast (in the back-scatter imaging mode of the scanning electron microscope) with respect to the alumina crystalline phase. In addition, no intermediate crystalline phases were detected on prolonged heating up to 1600° C with the alumina. According to the manufacturer's data, the viscosity of the 7059 glass over the conventional working range is shown in Fig. 1 with a softening point ($\log \eta = 7.6$) at 850° C and a flow point ($\log \eta = 5.0$) at 1025° C. The alpha-alumina starting powder had a median size of 3 $\mu$m and was dispersed with the powdered glass in methanol prior to drying and subsequent hot-pressing to full density.

### 2.2. Microstructure

Transmission electron microscopy using bright-field imaging and diffuse dark-field* techniques [1] showed the glass phase to be distributed uniformly throughout the microstructure and to wet both the alumina three-grain junctions and the two-grain interfaces. At the majority of two-grain junctions the thickness of the intergranular glass phase was constant but occasional evidence for anisotropic wetting behaviour and facetting was also observed (Fig. 2).

## 3. Creep measurements

The uniaxial creep properties of the material in air were studied at temperatures of 850, 950, 1050 and 1150° C using a constant load creep machine described in detail elsewhere [2]. The sample was in the form of a right-rectangle 9 mm long and a square cross-section (3 mm × 3 mm). The ends of the sample were accurately ground and diamond polished in a jig to ensure parallelism of the loading surfaces. In addition, the other surfaces of the samples were also diamond ground. The uniaxial strain was measured directly using an extensometer with single-crystal sapphire rods and employing a linear transducer. In this manner the contraction of the sample throughout the creep test was monitored. The densities of the samples were measured both prior to and at the termination of the creep tests. The technique, a pycnometer method using a mixture of diiodemethane and neothane [2], was capable of reproducing a den-

*An imaging mode in which non-crystalline regions appear bright and crystalline regions dark.

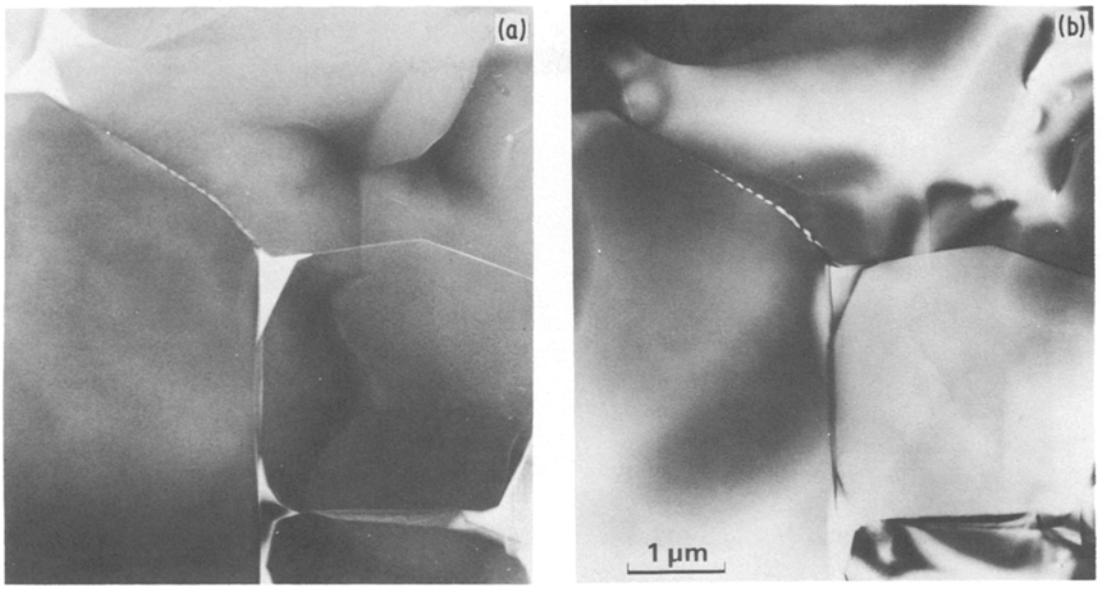


*Figure 2* Diffuse dark-field (a) and bright-field (b) transmission electron micrographs illustrating the continuous, intergranular nature of the glass phase along the two-grain and three-grain junctions of the alumina phase. The glass phase, appearing bright in the diffuse dark-field image, is concentrated at the three-grain junctions.

sity measurement to +0.01%. Three samples were tested for each temperature and stress level.

At all temperatures and applied stresses the plots of strain against time exhibited the conventional response regimes of primary, secondary (steady-state) and tertiary creep. However, in contrast to the behaviour of single-phase ceramics, the secondary regime was generally shorter than that of the tertiary regime, and in some tests was barely distinguishable. This was particularly marked at the higher applied stresses as shown by the curves of Fig. 3. One other unusual feature of the creep curves was that, when taken to failure, the fracture strain was smaller the larger the applied stress (Fig. 3).

The strain rate/stress response of the materials at the four test temperatures spanning the working range of the glass are represented in Fig. 4. The curves can be represented by the empirical relationship

$$\dot{\epsilon} = A\sigma^n$$

over the stress range 30 to 45 MPa. At the highest test temperature the material exhibited a stress exponent of ~ 2.8 whereas at the three lower temperatures of 850, 950 and 1050° C the stress exponent was considerably higher having a value of ~ 6.3. No region having a linear stress–strain rate behaviour was distinguished.

All the samples which did not rupture during the test exhibited a measurable increase in volume after compressive creep deformation as shown by the data of Fig. 5. (The horizontal error bars in the figure are a measure of the accuracy in measuring the length of the sample, whereas the vertical height of the symbols represents the accuracy of the density measurements.) That the volume increase was a manifestation of cavitation was confirmed by the observation by transmission electron microscopy of cavities at three-grain junctions such as is shown by the micrographs of Figs. 6 and

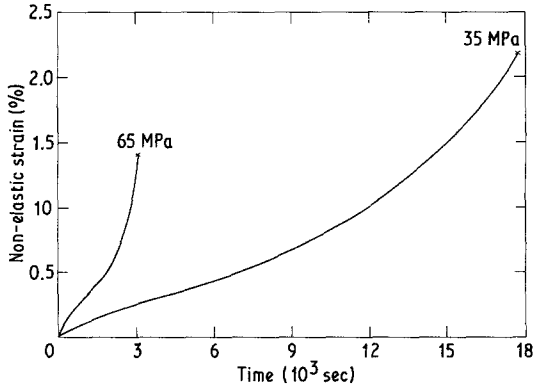


*Figure 3* Comparison of the true creep strain response of the alumina material at 1150° C for two different applied stresses.

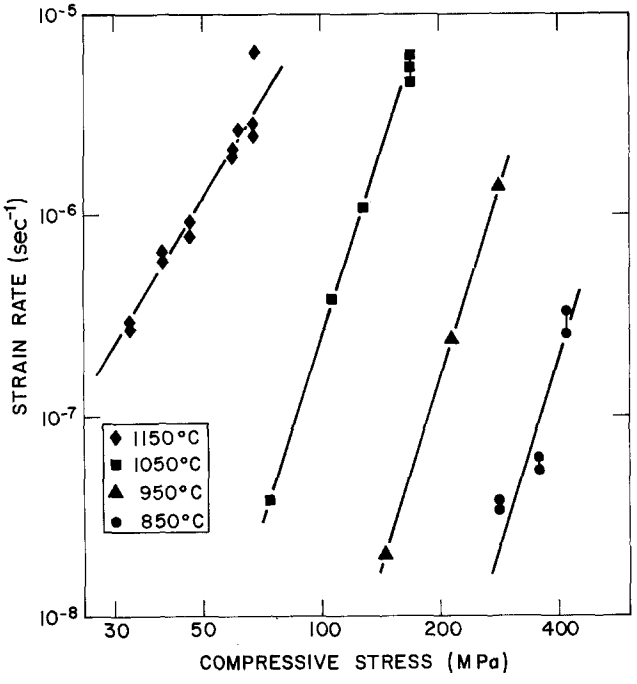


*Figure 4* The apparent steady-state creep rate as a function of compressive stress for the alumina-glass composite over the temperature range of 850 to 1150° C.

7. Fig. 6 reveals that the cavity forms within the glass phase at the triple grain junction suggesting that the cavity nucleated and grew within the glass phase. Cavitation was also evident from the change in appearance of the sample; before deformation the material was translucent but after deformation it had a whitish, opalescent character (Fig. 8). This behaviour was particularly striking under oblique polarized light illumination. Further evidence for cavitation comes from scanning electron micrographs of the sample surfaces after light polishing (with Jewellers Rouge). These also show that the number density of cavities is not uniform but

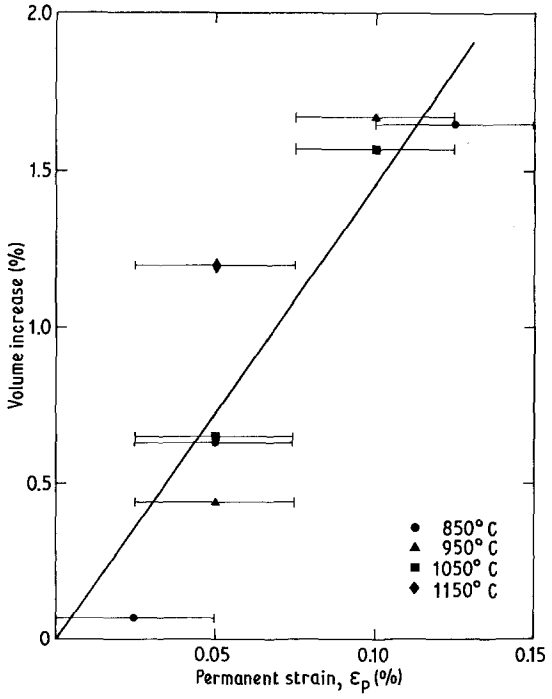


*Figure 5* Volume increase of the compressive creep samples as a function of the permanent strain experienced by the samples.

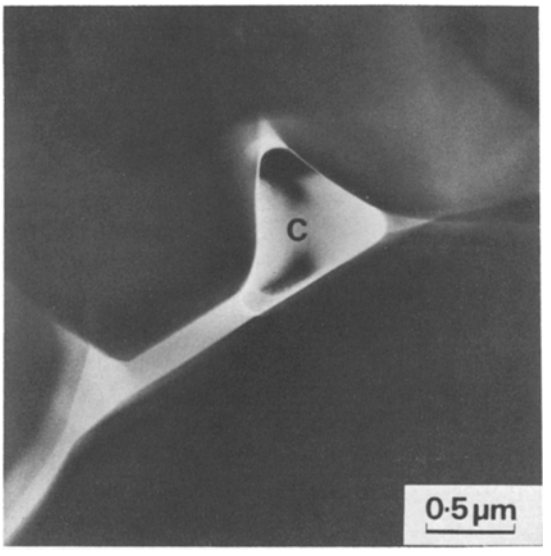


*Figure 6* Transmission electron micrograph illustrating the formation of a creep cavity, C, in the glass phase situated at a three-grain junction. The cavity appears to be totally lined by the glass phase. Diffuse dark-field image.

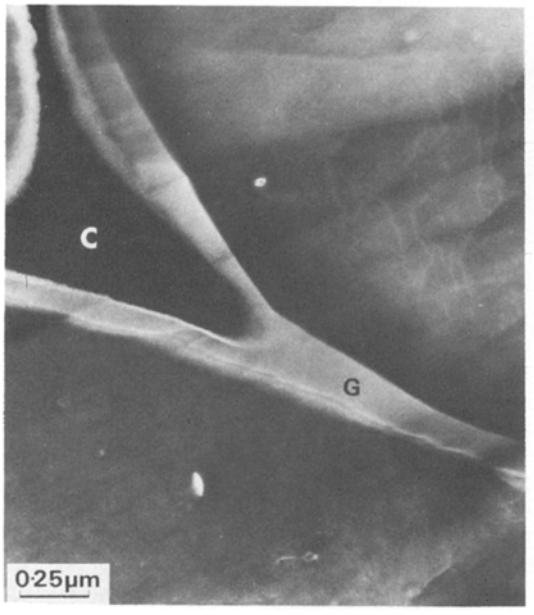


*Figure 7* Diffuse dark-field image of a cavity, C, at a three-grain junction growing into the two-grain channel of glass, G. The shape of the vapour/glass meniscus is particularly clear.

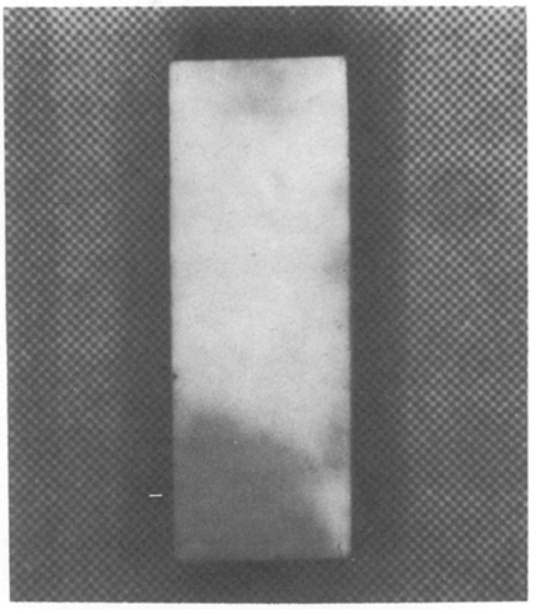

*Figure 8* Appearance of a sample after creep deformation into the secondary regime at 1150° C. Prior to testing the sample was a uniform grey but as deformation proceeded whitening developed due to the formation of internal cavities. Optical photograph.

rather that they are concentrated in bands (Fig. 9). At later stages in the deformation the bands are sufficiently well developed to be seen by eye (Fig. 10). Furthermore, the bands are associated with steps formed on the surface. The bands were usually oriented at ~ 20° to the loading direction.

A number of the creep tests were terminated by the catastrophic failure of the samples. In these cases the samples failed by shearing into two pieces along one of the bands of cracks. Away from the cracks the density of cavities was relatively small.

One further observation made of the surfaces of the crept samples, was that they had become roughened by the extrusion of glass from the surface. The extrusions could readily be seen by eye and by microscopy (Fig. 11).

## 4. Flexural strength

The flexural strength of the material was measured in four-point bending using both pre-cracked and un-cracked samples at temperatures up to 1250° C. The samples were in the form of rectangular bars 3 mm × 6 mm × 30 mm and in all cases the tensile surfaces and associated edges were diamond ground and polished to remove surface flaws and cracks prior to testing. Controlled pre-cracks were introduced after polishing by indentation with a Knoop hardness indentor. The results of the strength measurements made at a strain rate of 0.001 are shown in Fig. 12. As has been reported for a number of other ceramics containing a glass phase [3, 4] the strength of the samples falls off rapidly above a threshold temperature. No difference between the pre-cracked and un-cracked sample strengths could be detected although this has been reported for silicon nitride ceramics [3]. Above 950° C the load–elongation curves of all the samples exhibited distinct curvature.

The fracture surfaces of the samples fractured at temperatures above the threshold temperature of Fig. 12 were all similar as shown by the scanning electron micrographs in Fig. 13. The outlines of the alumina grains can be clearly seen, together with extensive cavitation between the grains and, particularly at the highest temperatures, islands of glass on the exposed grain faces. At the lower temperatures the glass is in the form of stringers whereas at the higher temperatures such morphological detail is lost and the glass has puddled. (The latter is attributed to slumping of the glass stringers at the test temperature and during the subsequent time on cooling.)

Observation in the scanning electron micro-

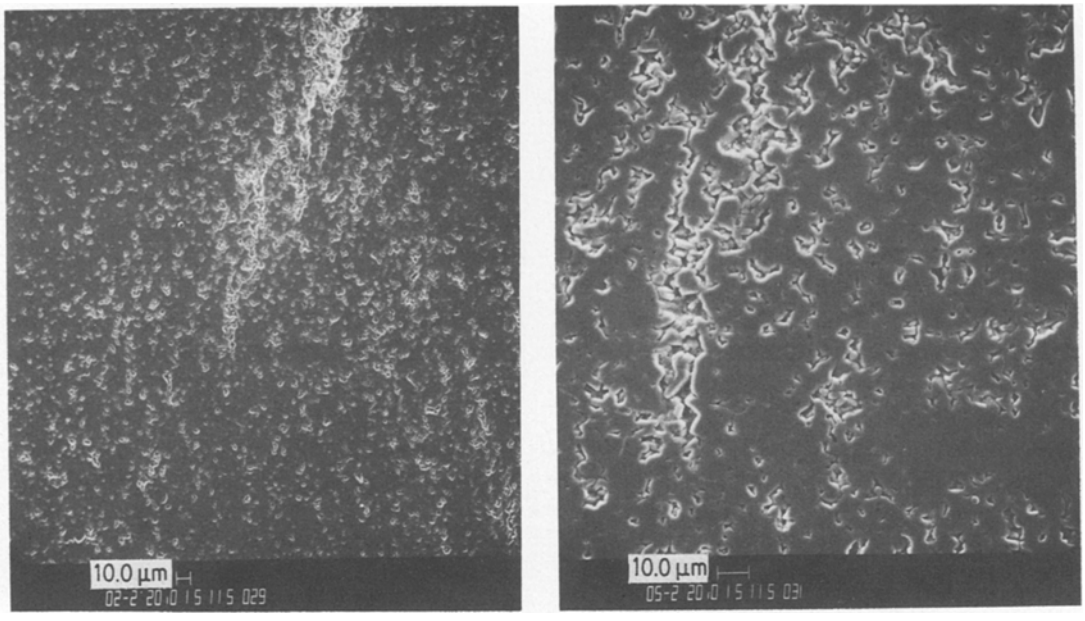


*Figure 9* Scanning electron micrographs of the surface of the sample shown in the previous figure, illustrating the inhomogeneous distribution of cavities and the fact that there is a propensity to form bands of cavities. The micrograph on the right is a magnification of that on the left.

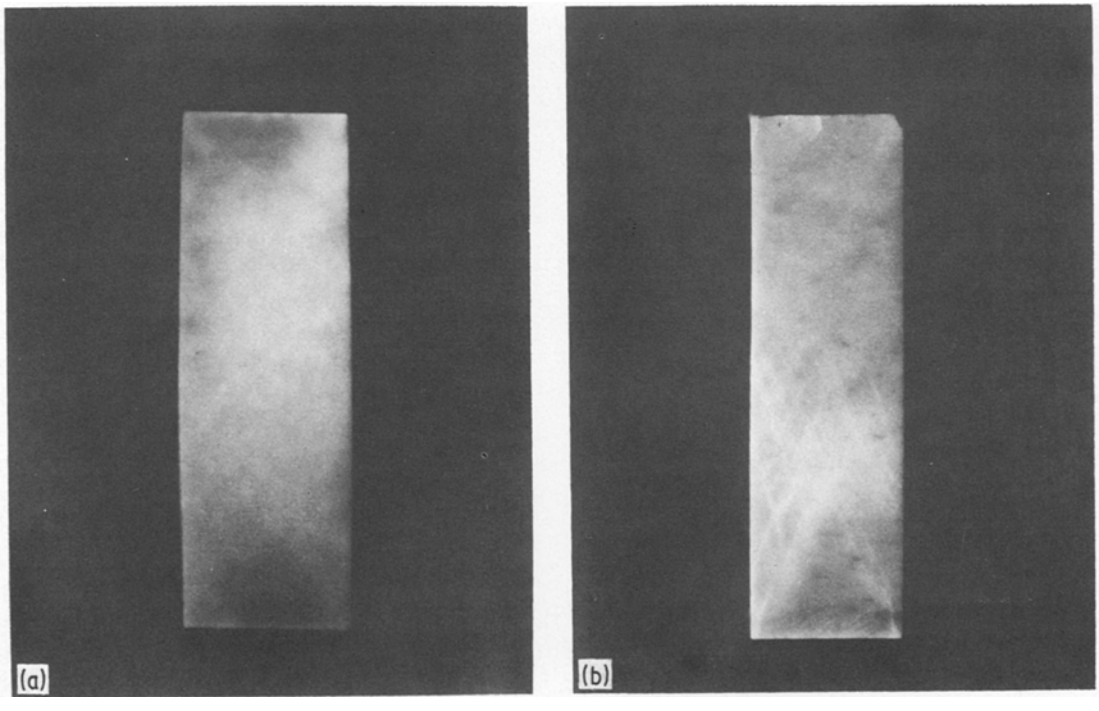


*Figure 10* Appearance of the material prior to final failure but after deformation well into the tertiary regime showing the macroscopic formation of cavity bands. Optical photographs under (a) normal illumination and (b) oblique lighting. The latter viewing conditions favour observation of the bands.

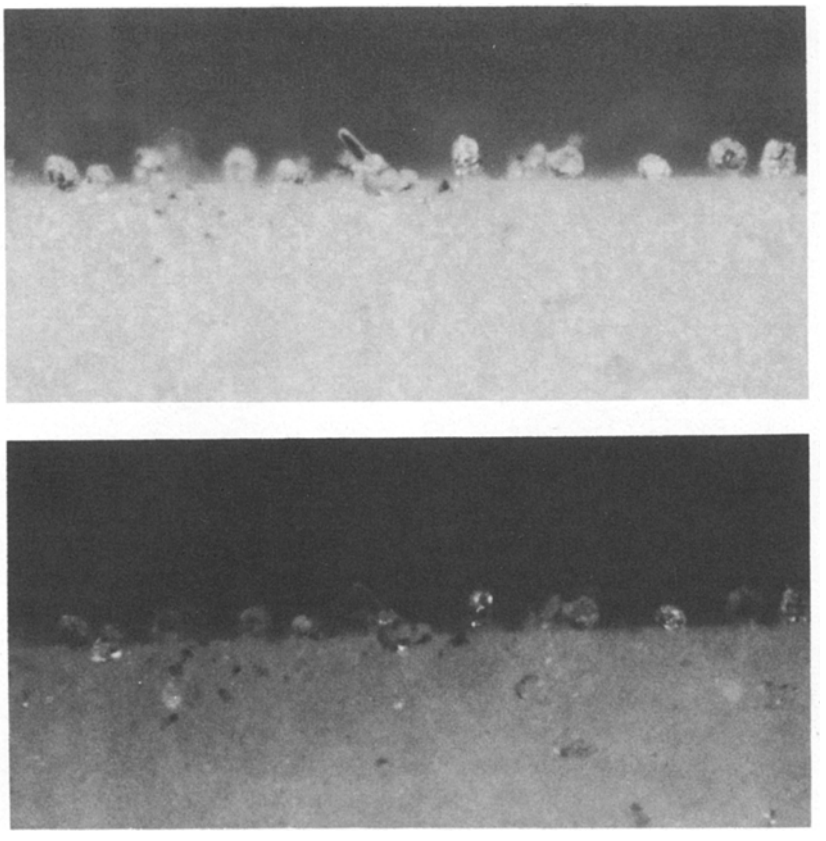

*Figure 11* Extrusions of glass on the surfaces of a crept sample as viewed by optical microscopy using normal (top) and oblique (bottom) lighting. Similar extrusions were visible on all the creep samples and on the tensile faces of the flexural test samples.

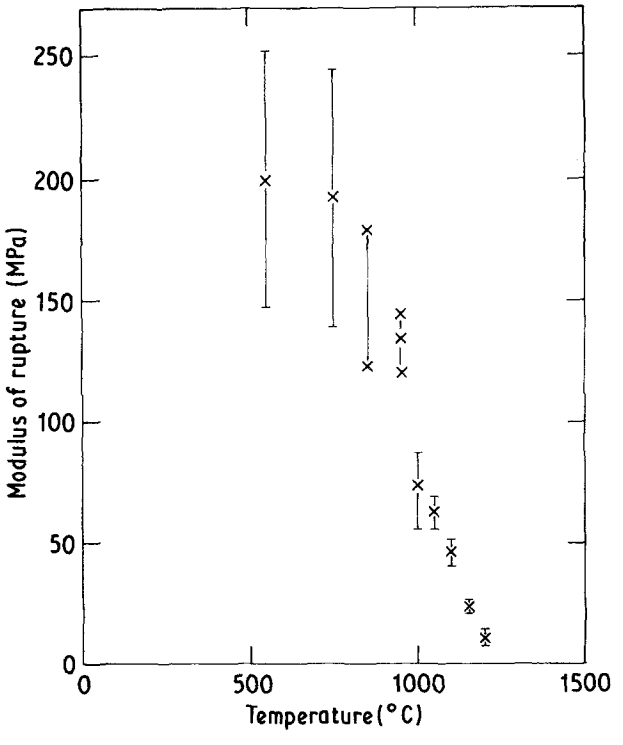


*Figure 12* Four-point modulus of rupture as a function of test temperature. No difference between the pre-cracked and un-cracked samples could be detected.

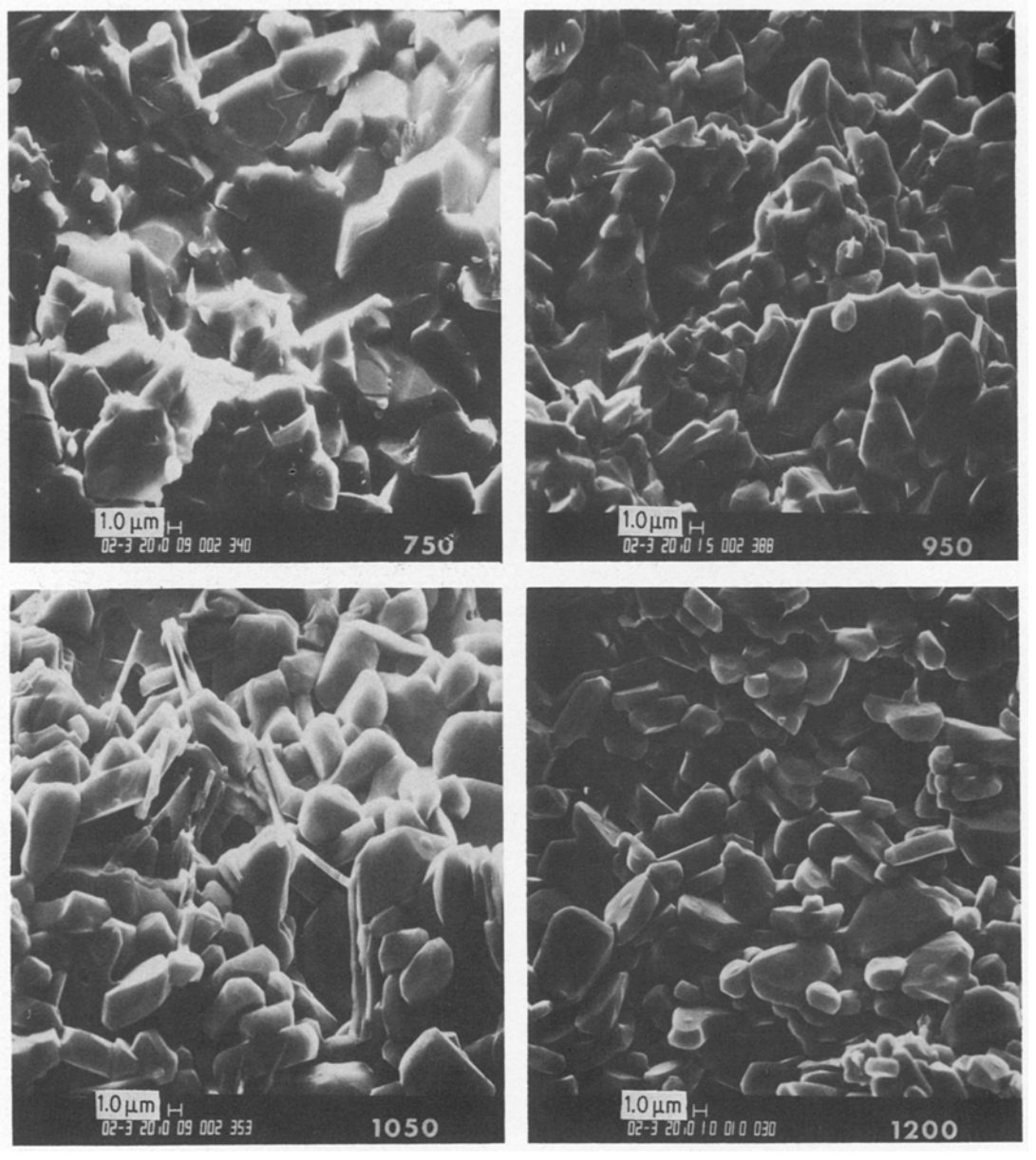


*Figure 13* Fracture surfaces of the samples broken in flexure at the temperatures indicated. As the test temperature is raised, viscous deformation of the glass phase becomes more evident and by 1200° C the individual grains can be easily distinguished by the glass having flowed from between the grains. Slumping of the glass may also be seen.

scope of the sides of the samples at the intersection with the fracture indicated that cavitation had also taken place on either side of the crack plane, but the extent was obscured by the extrusion of glass at the surfaces. Thus, to expose the cavitational zone for measurement the samples fractured at high temperature were broken at room temperature by loading a Knoop hardness indentor so that the lateral cracks propagated and intersected the high-temperature fracture surface perpendicularly (Fig. 14). (This approach was adopted in preference to cutting and polishing since polishing tends to fill in microstructural features with abrasive and debris thereby obscuring detail.) By this simple device it was possible to distinguish the extent of cavitation. The size of the cavitational zone was determined from scanning micrographs of the brittle fracture surface so produced with micrographs being recorded at successively larger distances from the high-temperature fracture. The

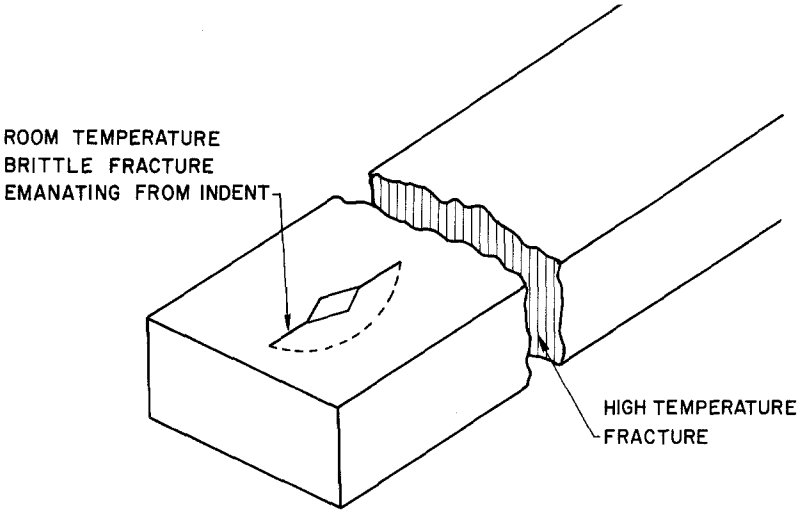


*Figure 14* Schematic diagram illustrating the method of extending a room-temperature, brittle fracture from a hardness indentation crack to expose the regions, including any cavitational zone, below a high-temperature fracture surface.

measured cavitational zone size (normalized by the average alumina grain size) as a function of test temperature, is shown in Fig. 15, and as can be seen is strongly temperature-dependent. As might be expected, the cavitational zone was not sharply delineated so the somewhat arbitrary criterion of a cavity number density, double that well removed from the fracture surface, was used in deciding whether or not a region was within the zone. The size of the error bars represent an estimate of the variability of the zone size from one position along the crack plane to another. No systematic variation in zone size with crack position was found.

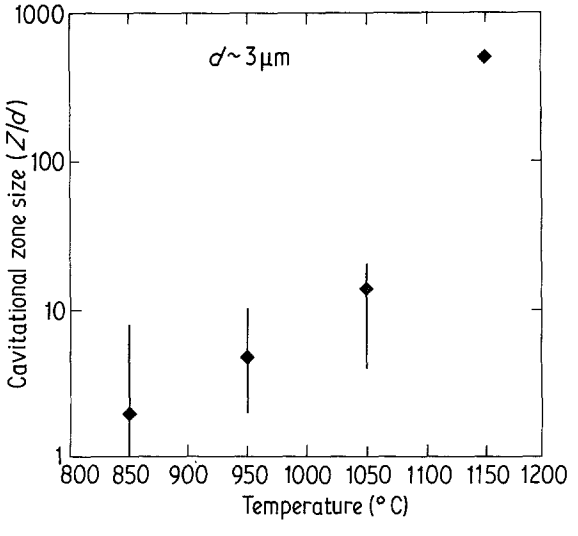


*Figure 15* Size of the measured cavitational zone produced by high-temperature fracture as a function of temperature. Size is normalized by the average grain size of the alumina.

The room-temperature fracture also enabled the morphology of the cavities to be observed. A particularly clear example is reproduced in the scanning micrograph of Fig. 16 recorded ~ 20 $\mu$m below the crack plane in the sample fractured at 1050° C. Cavities at the majority of three-grain junctions are evident. The shape of the cavity–glass interface can be seen since the room-temperature fracture in the intergranular glass phase has produced characteristic hackle features. The glass phase is also distinguishable on account of its higher back-scatter image contrast. Another example of the shape of the cavities is given by the micrograph of Fig. 17, which clearly shows the shape of the meniscus at the tip of the cavity.

## 5. Discussion

In the absence of existing theories describing the deformation of a material containing a viscous intergranular glass phase in terms of the properties of both the glass phase and the crystalline phase to evaluate the discussion here is limited to a phenomenological description of the processes involved during deformation. The principal finding of the study, and one clearly illustrated by the observations presented, is that the high-temperature deformation of polycrystalline alumina containing a small volume fraction of a liquid phase is dominated by cavitational processes within the glass phase. Cavitation is found to occur during both flexural deformation, creep and fracture.

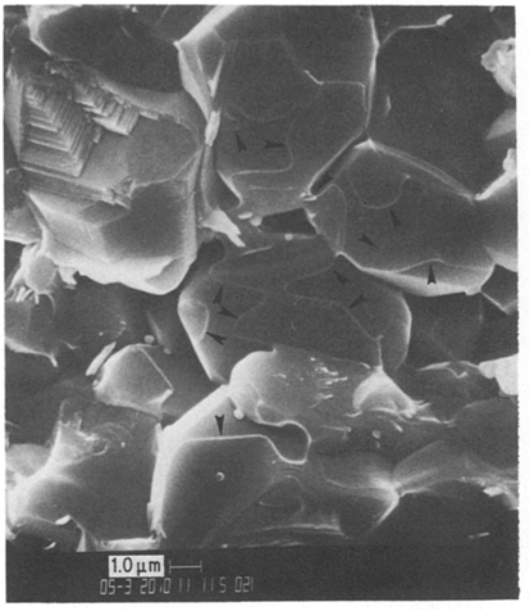


*Figure 16* Scanning electron micrograph of a portion of the cavitational zone produced at a temperature of 1050° C and exposed by a room-temperature brittle fracture. The micrograph reveals the shape and location of the cavities as well as the morphology of a number of the cavity meniscii (arrowed). Complete depletion of the majority of three-grain junctions has occurred together with the linking up of adjacent cavities. In the centre of the micrograph two cavity meniscii are approaching across a two-grain junction. They also exhibit a finger-like perturbation.


*Figure 17* Higher magnification image of the profile of an advancing cavity meniscus in which the shape of the vapour/glass interface can be seen particularly clearly.

Crack propagation during fracture at high temperatures is accompanied by cavitation with the formation of a cavitational zone around the crack. The size of this cavitational zone is strongly dependent on the viscosity of the intergranular glass phase, as shown by the data of Fig. 15. Direct comparison with theoretical estimates [5, 6] of the zone size is not strictly possible since the existing models have been concerned with the development of a cavitational zone ahead of the crack tip in terms of a known applied stress intensity, whereas the present measurements relate to a zone on either side of the crack plane in a conventional flexure test in which the stress intensity is unknown. However, if it is assumed that the zone is circular in shape at the crack tip, then, following Tsai and Raj [5] the zone size will be exponentially dependent on temperature in recognition that the viscosity of the glass phase decreases exponentially with temperature. Such a behaviour is in accord with the trend in the findings of Fig. 15. (The data of this figure have been used by Tsai and Raj (Fig. 15) as an experimental test of their model.)

The photomicrographs recorded from within the cavitational zone provide some insight as to how individual cavities form and then link up together. The sequence is much as envisaged by Evans and Rana [7] and more recently analysed by Marion *et al.* [8]. In these papers cavities are considered to form within the intergranular phase, principally at three and four grain junctions, and then grow by the progressive advance of the glass/vapour meniscus into, and along, the two-grain junctions until meeting a similarly growing cavity. Examination of the meniscus shapes in the micrographs indicate that the meniscii do not in all cases spread across the two-grain faces uniformly but rather exhibit finger-like perturbations. Such features could occur as a result of either the thickness of the two-grain channel being non-uniform or alternatively as a result of a flow instability as the cavity grows. The latter would be an example of the finger-like instabilities analysed by Fields and Ashby [9], and recently analysed, for the case of cavity advance, by Marion *et al.* [8]. On the basis of the scanning electron micrographs, cavitation would appear to be simply a phenomenon of viscous flow in the intergranular phase. In contrast, the observations made using transmission

electron microscopy, such as that of Fig. 7, suggest that solution-reprecipitation occurs concurrently. The simplest indication is that the cavities are significantly larger in size than the size of the original glass pockets at the three-grain and four-grain junctions. In addition, as illustrated by the shape of the cavity in Fig. 7, the width of the two-grain channel progressively changes in the immediate vicinity of the cavity, rather than being of reasonably constant thickness, as in Fig. 6, when the cavity is still confined to the size of the glass pocket.

Although the cavitational strain as a function of permanent strain in Fig. 5 suggests that the extent of cavitation is homogeneous during creep, both the visual appearance of the samples and the observations in the scanning electron microscope of the sample surfaces demonstrate that cavitation is microstructurally inhomogeneous and is, furthermore, localized into bands. Such bands can be discerned, with some difficulty, on the surfaces of the flexural test bars but they are particularly evident on the compressive creep samples as shown in the optical micrograph of Fig. 10. In appearance the bands are reminiscent of shear bands seen after plastic deformation of fully crystalline materials. They are also similar to the zones of fissures developed during the constrained fracture of rocks and described by Koide [10]. He observes that in the process of fracturing, a series of bands of shear fractures are created that, on microscopic examination, are seen to consist of a large number of individual, short microcracks. The same description may be used to describe the deformation bands seen in this work as can be gauged in examining the scanning electron micrograph of Fig. 9. The majority of the bands are, as mentioned in the previous section, inclined at an angle of 20° to the compression axis. The angle was approximately the same for all the temperatures for which the material was tested. According to existing theory, the angle of the shear bands is determined by the ratio of the deviatoric and dilatational stress. The term "shear bands" is believed to be appropriate, since the parts of the samples sheared apart when they were crept to rupture. The detailed microstructural development of the localization of brittle fractures into shear zones remains to be established for ceramics containing an intergranular viscous phase, although the general constitutive conditions for such localization phenomenon have been published for pressure-sensitive dilatant materials [11].

The non-linear strain rate/applied stress behaviour in creep deformation is consistent with the high-stress reponse of other ceramic materials reported in the literature, particularly those containing a large volume fraction of intergranular phase. According to established beliefs, the existence of a stress exponent different to unity is interpreted to imply that the deformation is not diffusion-controlled. However, as pointed out by Lange *et al.* [2], the value of the creep exponent calculated is not uniquely defined by the deformation processes when cavitational damage occurs concurrently but rather is non-linearly dependent on the volume fraction of intergranular phase present in the microstructure, its viscosity and the deformation time. Also, as shown by the elegant experiments of Pharr and Ashby [12], a linear creep exponent can only be expected if the crystalline phase is soluble in the intergranular phase. More generally, an exponent of unity will only be exhibited if the solubility in the intergranular phase is sufficiently large for solution-reprecipitation creep to accommodate the stresses that would otherwise cause cavitational creep.

The observation of extruded glass on the surfaces of both the creep and the flexural test samples has not, as far as the author is aware, been reported previously. The observation, however, is consistent with the suggestion by Raj that the "pore" pressure in the intergranular glass phase, which corresponds to the net hydrostatic pressure in the material, exceeds the ambient pressure.

The observations presented here are consistent with the following picture of how ceramics containing a viscous intergranular glass phase deform at high temperature: as the material is loaded cavities nucleate at three-grain and four-grain junctions and grow within the intergranular phase by the viscous flow of the glass into adjoining channels until they deplete the pockets of all but a wetting film of glass (Fig. 6). The cavities then advance into the two-grain junction channels (Fig. 7) until they meet with a similarly growing cavity at an adjacent three-grain junction. The vapour/glass meniscus of the cavity may advance across the two-grain channel in either a uniform manner or become unstable and exhibit finger-like perturbations. Although less definite evidence for its occurrence is available mass transport is taking place by solution-reprecipitation concurrent with that of viscous flow. The growth of a cavity, and

in particular its growth linking it to another, appears to be biased by the presence of other, adjacent cavities in such a way that together they form concentrated bands of cavities. At a later stage these bands may represent the first stages in the formation of a macroscopic crack.

## 6. Conclusions

The high-temperature creep and flexural deformation of a model alumina composite ceramic containing 10 vol% of a well characterized glass have been investigated from 850 to 1250° C; a temperature range in which the glass softens from its "softening" point to well into its "working" range. At these temperatures the deformation of the alumina material is shown to be governed by the visco-elastic deformation of the glass phase. The principal mode of deformation is a damage mechanism in which cavities form in the intergranular glass phase and grow until they become interconnected. The cavities form inhomogeneously throughout the microstructure and accumulate in bands that appear to later develop into cracks or shear bands. In addition, as a crack propagates through the material at high temperature it forms a cavitational zone on either side. Measurements of the size of the cavitational zone, made using scanning microscopy observations, recorded from a room-temperature fracture intercepting the high-temperature fracture surface, are presented as a function of temperature. Furthermore, microstructural evidence is presented to show how cavities, formed at three-grain junctions, grow along two-grain junctions and subsequently interconnect to create what is presumed to be a critical flaw.


## Acknowledgements

It is a pleasure to acknowledge invaluable discussions with A. G. Evans, F. F. Lange, R. Raj and S. M. Wiederhorn during the course of this work. The author is also indebted to the Rockwell International Independent Research and Development Program for support of the experimental phases of the investigation.


## References


1. D. R. CLARKE, *Ultramicroscopy* **4** (1979) 33.
2. F. F. LANGE, D. R. CLARKE and B. I. DAVIS, *J. Mater. Sci.* **15** (1980) 601.
3. R. K. GOVILA, *J. Amer. Ceram. Soc.* **63** (1980) 319.
4. K. JAMES and K. H. G. ASHBEE, *Prog. Mat. Sci.* **21** (1975) 1.
5. R. L. TSAI and R. RAJ, *Acta Metall.* **30** (1982) 1043.
6. D. S. WILKINSON and V. VITEK, *ibid.* **30** (1982) 1723.
7. A. G. EVANS and A. RANA, *ibid.* **28** (1980) 129.
8. J. E. MARION, A. G. EVANS, M. D. DRORY and D. R. CLARKE, *ibid.* **31** (1983) 1445.
9. R. J. FIELDS and M. F. ASHBY, *Phil. Mag.* **33** (1976) 33.
10. H. KOIDE, *Soc. Mining Geol. Jpn. special issue* **3** (1971) 107.
11. J. W. RUDNICKI and J. R. RICE, *J. Mech. Phys. Solids* **23** (1975) 371.
12. G. M. PHARR and M. F. ASHBY, *Acta Metall.* **31** (1983) 129.



*Received 16 April*
*and accepted 23 May 1984*